

An Analytical Derivation of a Popular Approximation of the Voigt Function for Quantification of NMR Spectra

Stephen D. Bruce,* John Higinbotham,* Ian Marshall,† and Paul H. Beswick‡

*School of Mathematical and Physical Sciences, Napier University, 10 Colinton Road, Edinburgh, EH10 5DT, Scotland; †Department of Medical Physics and Medical Engineering, The University of Edinburgh, Western General Hospital, Crewe Road, Edinburgh, EH4 2XU, Scotland; and

‡School of Life Sciences, Napier University, 10 Colinton Road, Edinburgh, EH10 5DT, Scotland

Received January 19, 1999; revised June 25, 1999

The approximation of the Voigt line shape by the linear summation of Lorentzian and Gaussian line shapes of equal width is well documented and has proved to be a useful function for modeling *in vivo* ¹H NMR spectra. We show that the error in determining peak areas is less than 0.72% over a range of simulated Voigt line shapes. Previous work has concentrated on empirical analysis of the Voigt function, yielding accurate expressions for recovering the intrinsic Lorentzian component of simulated line shapes. In this work, an analytical approach to the approximation is presented which is valid for the range of Voigt line shapes in which either the Lorentzian or Gaussian component is dominant. With an empirical analysis of the approximation, the direct recovery of T_2 values from simulated line shapes is also discussed. © 2000 Academic Press

Key Words: Voigt; approximation; NMR spectroscopy; quantification; modeling.

INTRODUCTION

Marshall *et al.* (1) and Friese *et al.* (2) describe the limitations of using fixed line shape models for accurate quantification of *in vitro* and *in vivo* NMR spectra of human brain metabolites. Although metabolite signals may be intrinsically monoexponential, imperfect shimming and susceptibility variations cause a spread of resonant frequencies within the spectroscopic volume of interest. For each metabolite resonance, the free induction decay (FID) will contain a roughly normal distribution of frequencies which can be pragmatically approximated by a Gaussian function. The metabolite line shapes resulting from the Fourier transformation (FT) of the time domain data will be a Gaussian broadening (convolution) of the intrinsically Lorentzian peaks. Such a convolution is well known to produce a Voigt line shape, a familiar profile in spectral line shape analyses (3–5). The normalized Voigt line shape (6) as a function of frequency f , is given as

$$V(f) = \frac{2\mu^2}{\pi^{3/2}w_L} \int_{-\infty}^{+\infty} \frac{\exp(-\zeta^2)}{\mu^2 + (q - \zeta)^2} \cdot d\zeta, \quad [1]$$

where w_L and w_G are the Lorentzian and Gaussian full widths at half maximum height (FWHM), and where

$$w_L = \frac{1}{\pi T_2}, \quad \mu = \sqrt{\ln 2} \left(\frac{w_L}{w_G} \right),$$

$$\zeta = \frac{2\sqrt{\ln 2} f'}{w_G}, \quad q = \frac{2\sqrt{\ln 2} (f - f_0)}{w_G},$$

where f_0 is the frequency at the center of the resonance, T_2 is the transverse relaxation time of the metabolite under investigation, and where f' is the frequency shift of the functions in the convolution integral (i.e., the variable of integration).

The proportion of Lorentzian and Gaussian contributions to the Voigt function is characterized by the Voigt parameter a , which is defined as

$$a = \frac{w_L}{w_G} \quad [2]$$

so that as $a \rightarrow \infty$, the Lorentzian component is dominant; at $a = 1$, there is an equal contribution from the Lorentzian and Gaussian components; while as $a \rightarrow 0$, the Gaussian component is dominant.

A common method of quantifying NMR spectra is to computer fit the experimental data using a model function whose component parameters are optimized in an iterative manner until the squared difference between the experimental data and the model data is minimized (nonlinear least squares fitting). Use of the exact Voigt function as a model would require the calculation of Eq. [1] for each data point in the spectrum, within each iteration of the fitting process. The computational burden therefore scales as n^2 , where n is the number of data points. Although within modern computing capabilities such intensive computing would present an unnecessary time burden when analyzing multiple spectra, such as in spectroscopic (chemical shift) imaging, where typically, an array of 8×8 spectra may be available from a subject.

Previously, accurate Voigt approximations were developed (3, 5, 7–9) and one such approximation, $V'(f)$ utilizes a linear combination of normalized Lorentzian $L(f)$, and Gaussian $G(f)$, functions given as

$$V'(f) = a[rL(f) + (1 - r)G(f)], \quad [3]$$

where a is the area of the combined function and r is the fractional parameter which varies the relative contributions of $L(f)$ and $G(f)$.

Since Eq. [3] is computed only once for each data point, the computational burden will scale linearly with the number of data points, n . The approximation is therefore a more convenient model for multiple spectra analysis where it is desirable to minimize the computational time, providing the simpler model offers a negligible loss in accuracy.

The normalized forms of Lorentzian and Gaussian functions are given as

$$L(f) = \frac{2}{\pi w_L} \frac{1}{1 + \left(\frac{f - f_0}{w_L/2}\right)^2} \quad [4]$$

$$G(f) = \frac{2}{w_G} \sqrt{\frac{\ln 2}{\pi}} \exp\left[-\left(\frac{f - f_0}{w_G/2\sqrt{\ln 2}}\right)^2\right]. \quad [5]$$

In practice, the FWHM of the Lorentzian and Gaussian components w_L and w_G are restricted so as to be identical. This common width, w is thus also the FWHM of the approximated Voigt line shape. This restriction of the width, along with the approximation itself has been discussed by Kielkopf (3) who showed that the resulting errors were less than 1.2% in terms of line shape amplitude. Using simulated spectra (described later) to generate a comprehensive range of Voigt lineshapes, we have shown (10) that the corresponding peak area errors are less than 0.72% (Fig. 1).

Equation [3] can be readily incorporated into a standard nonlinear least squares fitting routine to return the model parameters a , r , f , and w . At the two extremes this model is exactly correct so that when $r = 0$, $V'(f)$ is purely Gaussian and when $r = 1$, $V'(f)$ is purely Lorentzian. Values of r in between produce approximated Voigt line shapes corresponding to the varying contributions from $L(f)$ and $G(f)$.

THEORY

The usefulness of Fourier techniques when dealing with convolution processes lies in the convolution theorem so that if a convolution is to be performed in the frequency domain then, by transforming the functions into the time domain, the process becomes a much simpler one of multiplication (11).

Applying an inverse FT to Eq. [4] gives a decaying exponential defined for $t > 0$ as

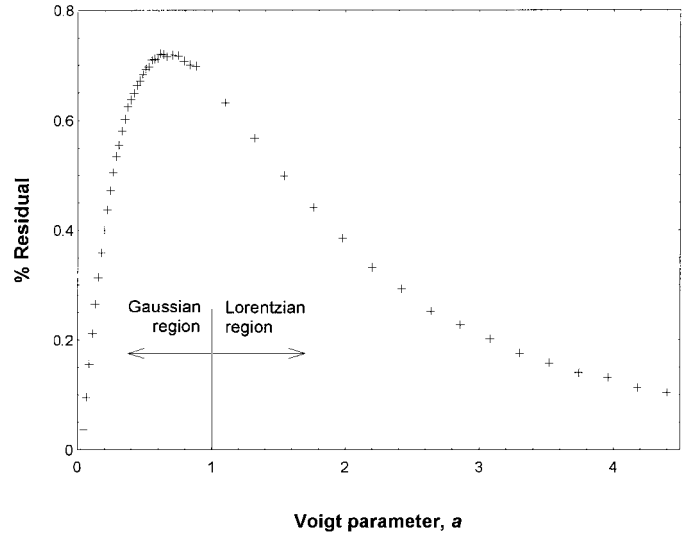


FIG. 1. Use of the approximation as a model function to determine peak areas results in errors of less than 0.72% over a range of Voigt line shapes. The peak area residual as a function of the Voigt parameter a , is plotted.

$$l(t) = \exp(-\pi w_L t). \quad [6]$$

Applying an inverse FT to Eq. [5] gives a Gaussian decay defined for $t > 0$ as

$$g(t) = \exp\left[-\left(\frac{\pi w_G t}{2\sqrt{\ln 2}}\right)^2\right]. \quad [7]$$

The actual Voigt function in the time domain, $\nu(t)$ is thus given as

$$\nu(t) = l(t) \cdot g(t). \quad [8]$$

From Eqs. [6], [7], and [8] we obtain

$$\nu(t) = \exp(-\pi w_L t) \exp\left[-\left(\frac{\pi w_G t}{2\sqrt{\ln 2}}\right)^2\right]. \quad [9]$$

The significant part of the NMR signal occurs at the beginning of the FID ($t < T_2$) where the signal to noise ratio is large, so Eq. [9] is now expanded as an exponential series limited to t^2 , as any further expansions to include higher order terms of t do not reveal any additional useful information. The actual Voigt function now becomes

$$\nu(t) = 1 - (\pi w_L)t + \left(\frac{\pi^2 w_L^2}{2} - \frac{\pi^2 w_G^2}{4 \ln 2}\right)t^2 + \dots \quad [10]$$

The Voigt approximation in the time domain, $\nu'(t)$ is given by a linear sum

$$\nu'(t) = rl(t) + (1 - r)g(t). \quad [11] \quad \text{Similarly, equating coefficients of } t^2 \text{ we obtain}$$

Denoting the Lorentzian and Gaussian FWHMs in the approximation as w'_L and w'_G , respectively, so that from Eqs. [6], [7], and [11], and expanding as an exponential series up to terms in t^2 , we obtain

$$\begin{aligned} \nu'(t) = & r[1 - \pi w'_L t + \frac{1}{2}(\pi w'_L t)^2 + \dots] \\ & + (1 - r)\left[1 - \left(\frac{\pi w'_G t}{2\sqrt{\ln 2}}\right)^2 + \dots\right]. \end{aligned} \quad [12]$$

The ratio of the Lorentzian and Gaussian FWHMs comprising the approximation a' , is given as

$$a' = \frac{w'_L}{w'_G}. \quad [13]$$

We recall that the approximation detailed by Kielkopf (3) and investigated previously by the authors (10) restricted the FWHMs of the Lorentzian and Gaussian components to be equal so that $w'_L = w'_G = w$, which corresponds to the case where $a' = 1$. The approximation given in Eq. [12] now becomes

$$\begin{aligned} \nu'(t) = & r[1 - (\pi w)t + \frac{1}{2}(\pi w)^2 t^2 + \dots] \\ & + (1 - r)\left[1 - \left(\frac{\pi w t}{2\sqrt{\ln 2}}\right)^2 + \dots\right]. \end{aligned} \quad [14]$$

Lorentzian Limit of the Voigt Function

As the actual Voigt line shape becomes more Lorentzian in nature,

$$w_L \gg w_G \quad \text{i.e., } \frac{1}{a} \rightarrow 0.$$

Expressing the general case of the Voigt function in Eq. [10] in terms of the Lorentzian FWHM w_L , while retaining terms up to a^2 to ensure that w remains a function of a , we have

$$\nu(t) = 1 - (\pi w_L)t + \left(\frac{\pi^2 w_L^2}{2} - \frac{\pi^2 w_L^2}{4a^2 \ln 2}\right)t^2 + \dots \quad [15]$$

As there are now only two unknown variables, deriving expressions for r and w in terms of w_L and a can be achieved by equating coefficients of t and t^2 in Eqs. [14] and [15].

Equating coefficients of t we obtain

$$r = \frac{w_L}{w}. \quad [16]$$

$$\frac{\pi^2 w_L^2}{2} - \frac{\pi^2 w_L^2}{4a^2 \ln 2} = \frac{r \pi^2 w^2}{2} + \frac{r \pi^2 w^2}{4 \ln 2} - \frac{\pi^2 w^2}{4 \ln 2}.$$

Hence,

$$\left(\frac{1}{2 \ln 2}\right)w^2 - \left(w_L + \frac{w_L}{2 \ln 2}\right)w + \left(1 - \frac{1}{2a^2 \ln 2}\right)w_L^2 = 0.$$

Using the quadratic method we obtain the two possible solutions

$$w = w_L \left[\left(\frac{1}{2} + \ln 2\right) \pm \sqrt{\left(\frac{1}{2} - \ln 2\right)^2 + \frac{1}{a^2}} \right]. \quad [17]$$

Only the root involving the positive square root gives the correct limit of w_L for $a \rightarrow \infty$, and the correct range of $r(0 - 1)$, so that

$$w = w_L \left[\left(\frac{1}{2} + \ln 2\right) + \sqrt{\left(\frac{1}{2} - \ln 2\right)^2 + \frac{1}{a^2}} \right]. \quad [18]$$

Substituting for w into Eq. [16] we obtain

$$r = \frac{1}{\left[\left(\frac{1}{2} + \ln 2\right) + \sqrt{\left(\frac{1}{2} - \ln 2\right)^2 + \frac{1}{a^2}} \right]}. \quad [19]$$

Gaussian Limit of the Voigt Function

As the Voigt lineshape becomes more Gaussian in nature,

$$w_G \gg w_L \quad \text{i.e., } a \rightarrow 0.$$

Expressing the general case of the Voigt function in Eq. [10] in terms of the Gaussian FWHM w_G , we have

$$\nu(t) = 1 - (\pi a w_G)t + \left(\frac{\pi^2 a^2 w_G^2}{2} - \frac{\pi^2 w_G^2}{4 \ln 2}\right)t^2 + \dots$$

Discarding higher order terms of a we have

$$\nu(t) = 1 - (\pi a w_G)t - \left(\frac{\pi^2 w_G^2}{4 \ln 2}\right)t^2. \quad [20]$$

As there are now only two unknown variables, deriving expressions for r and w in terms of w_G and a can be achieved by equating coefficients of t and t^2 in Eqs. [14] and [20], respectively.

Equating coefficients of t and using Eq. [2], we obtain

$$r = \frac{aw_G}{w} = \frac{w_L}{w}. \quad [21]$$

Similarly, equating coefficients of t^2 we obtain

$$-\frac{\pi^2 w_G^2}{4 \ln 2} = \frac{r \pi^2 w^2}{2} + \frac{r \pi^2 w^2}{4 \ln 2} - \frac{\pi^2 w^2}{4 \ln 2}.$$

Hence,

$$w^2 - aw_G(1 + 2 \ln 2)w - w_G^2 = 0. \quad [22]$$

Using the quadratic method and discarding terms in a^2 , we obtain the two possible solutions

$$w = w_G \left[a \left(\frac{1}{2} + \ln 2 \right) \pm 1 \right]. \quad [23]$$

Only the root involving the positive sign gives the correct limit of w_G for $a \rightarrow 0$, so that using Eq. [2] we find

$$w = w_L \left(\frac{1}{2} + \ln 2 + \frac{1}{a} \right). \quad [24]$$

Substituting for w into Eq. [21], we have

$$r = \frac{1}{\left(\frac{1}{2} + \ln 2 + \frac{1}{a} \right)}. \quad [25]$$

METHOD

Software for the generation of synthetic data and frequency domain modeling was written in-house using the ‘‘C’’ language on a SPARC-10 workstation (SUN Microsystems, Mountain View, CA) running UNIX. To generate actual Voigt functions, a Fourier transform is applied to the multiplication of an exponentially decaying sinusoid, consisting of 2048 data points at 1-ms intervals, by a Gaussian decay. A range of Voigt parameters was achieved by fixing T_2 at 50 ms (Lorentzian FWHM, $w_L = 6.37$ Hz) and varying the contribution of the Gaussian decay.

The resulting synthetic spectra, consisting of single peaks, were computer fitted using a Levenberg–Marquardt nonlinear least squares fitting routine (12) using the Voigt approximation in Eq. [3] as the model function. Initial estimates of the model parameters were determined automatically and convergence to the parameter values was deemed to have been achieved when the change in the parameter values was less than 1 in 10^7 . To restrict the fractional parameter r to the physically meaningful

range of 0 to 1, the model used an internal parameter R with $r = \exp(-|R|)$. For satisfactory convergence to accurate parameter values, we found that r is required to be initially set at 100% Lorentzian.

The peak areas of the synthetic spectra and the modeled spectra were determined by a simple summation of the data points comprising the peaks, with a peak area residual computed for each point. For *in vitro* and *in vivo* spectra, however, overlapping peaks severely limit integration so peak areas are taken directly from the fitted peak area parameter.

RESULTS

The accuracy of the Voigt approximation is presented in Fig. 1, where the Voigt parameter a is plotted against the peak area residual. The derivation is effective in the range of Voigt functions where either Lorentzian or Gaussian effects dominate, and manifests itself as relationships between the parameters in the actual Voigt function and those in the approximation.

In the Lorentzian dominated region ($a > 1$), Eq. [18] expresses the FWHM of the Voigt approximation w in terms of the FWHM of the Lorentzian contribution to the actual Voigt function w_L , and the Voigt parameter a , whereas Eq. [19] expresses the fractional parameter r , only in terms of the Voigt parameter a . The accuracy of these expressions is demonstrated in Figs. 2a and 2b, which compare w and r as returned by the fitting routine on synthetic data, with w and r as calculated from Eqs. [18] and [19], respectively. The difference between the expression for the common line width w given in Eq. [18] and the value returned by the fitting routine is 0.18% in the extreme Lorentzian region ($a = 440$), and this value increases steadily so that when $a = 1.1$, the difference is 22.9% (Fig. 2a). Similarly, the difference between the fractional parameter r , given in Eq. [19], and the value returned by the fitting routine is 0.13% in the extreme Lorentzian region ($a = 440$) and this value increases steadily so that when $a = 1.1$, the difference is 26.4% (Fig. 2b).

In the Gaussian dominated region ($a < 1$), Eq. [24] expresses w in terms of the FWHM of the Lorentzian contribution to the actual Voigt function w_L , and the Voigt parameter a , and Eq. [25] expresses r in terms of a alone. The accuracy of these expressions is demonstrated in Figs. 3a and 3b, which compare w and r as returned by the fitting routine on synthetic data, with w and r as calculated from Eqs. [24] and [25], respectively. The difference between the expression for the common line width w given in Eq. [24] and the value returned by the fitting routine is 1.5% in the extreme Gaussian region ($a = 0.022$) and this value increases steadily so that when $a = 0.53$, the difference is 24.7% (Fig. 3a). The difference between the fractional parameter r given in Eq. [25] and the value returned by the fitting routine is between 30 and 33% over the bulk of the Gaussian region (Fig. 3b).

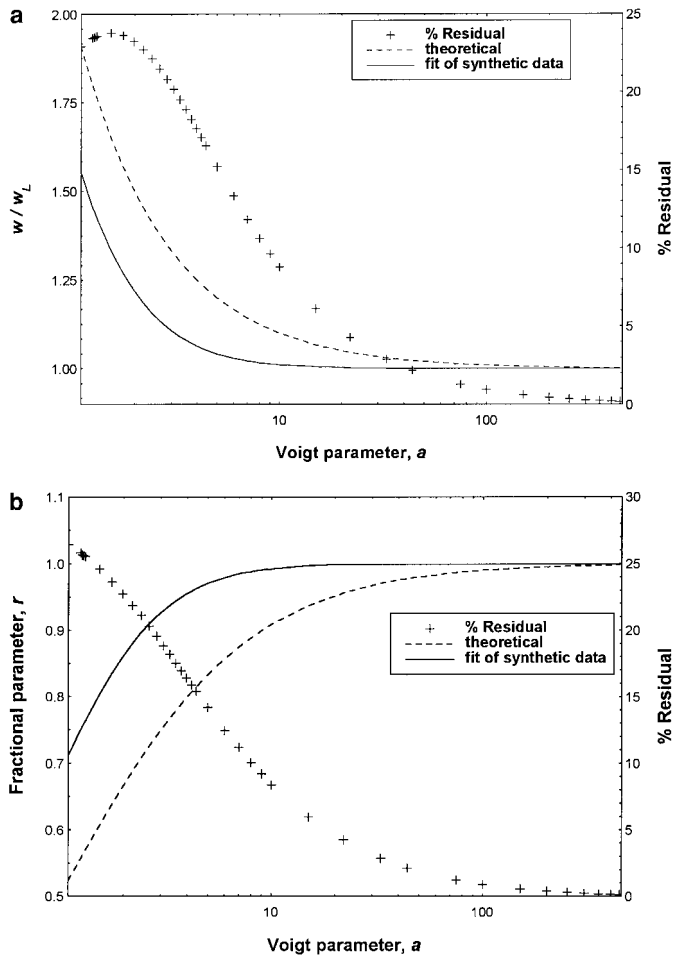


FIG. 2. Illustration of the accuracy of the derivation in the Lorentzian limit of Voigt line shapes. (a) Model parameter w , the line width: Plot of the theoretical w (Eq. [18]), actual w (returned by the fitting routine on synthetic data) and the corresponding residual, as a function of the Voigt parameter a . Both line widths are normalized to the underlying Lorentzian width w_L . (b) Model parameter r , the fractional parameter: Plot of the theoretical r (Eq. [19]), actual r (returned by the fitting routine on synthetic data) and the corresponding residual, as a function of the Voigt parameter a .

DISCUSSION

In spin echo experiments, estimating the T_2 values (and hence Lorentzian line widths) of metabolites usually requires spectroscopy measurements to be repeated with at least five different echo times in order that there are enough data points to accurately model the decay rate of the signal intensities. It would be of value to reduce the time of such experiments by directly recovering the underlying Lorentzian line widths of experimental line shapes. The following empirical analysis of the approximation as a model function discusses the possibility of such a recovery from the fitted model parameters.

Wertheim *et al.* (8) provided a graph, plotting the parameters $(1 - r)$ against w_G/w_V , where w_V is the FWHM of the experimental line shape. Although w_V is unknown, it is mod-

eled in the fitting routine by w , accurate to within 0.37% over a large range of Voigt parameters, therefore w_G/w was plotted against $(1 - r)$. To obtain an empirical relationship for w_G , a curve-fitting facility with a suggested equation $(1 - r) = k(w_G/w)^x$ was applied to the plot to determine k and x (Fig. 4). Using a nonlinear least squares fit, k and x were found to be 0.97 and 2.3, respectively, giving

$$w_G = w \left(\frac{1 - r}{0.97} \right)^{0.43} \quad [26]$$

The accuracy of Eq. [26] in the Gaussian region ($a < 1$) is within 1% and then drops through the Lorentzian region ($a > 1$) so that when $a = 10$, the accuracy is around 26%.

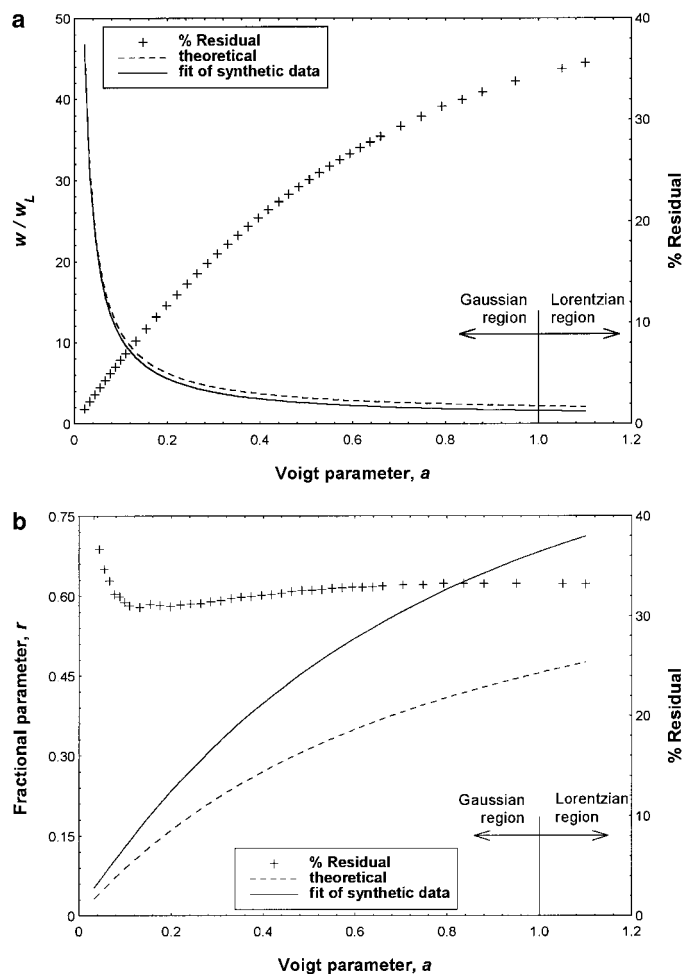


FIG. 3. Illustration of the accuracy of the derivation in the Gaussian limit of Voigt line shapes. (a) Model parameter w , the line width: Plot of the theoretical w (Eq. [24]), actual w (returned by the fitting routine on synthetic data) and the corresponding residual, as a function of the Voigt parameter a . Both line widths are normalized to the underlying Lorentzian width w_L . (b) Model parameter r , the fractional parameter: Plot of the theoretical r (Eq. [25]), actual r (returned by the fitting routine on synthetic data) and the corresponding residual, as a function of the Voigt parameter a .

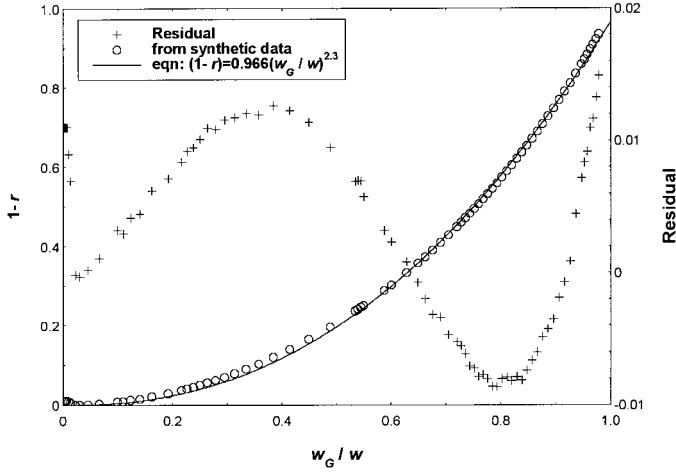


FIG. 4. Determination of an empirical expression for w_G , which is the line width of Gaussian component that broadens the intrinsic Lorentzian line shape, resulting in actual Voigt line shapes. The expression is in terms of model parameters returned by the fitting routine: w , the model line width and r , the fractional parameter.

Based on a table of standard Voigt profiles, the plotted results of Van de Hulst and Reesinck (4), were fitted by Whiting (9) to obtain the empirical expression

$$w_V = \frac{1}{2} [w_L + \sqrt{w_L^2 + 4w_G^2}]. \quad [27]$$

Equation [27] is accurate to within 1% and since w_G can be obtained from Eq. [26] and w can be substituted for w_V with sufficient accuracy, w_L can now be obtained from

$$w_L = \frac{w^2 - w_G^2}{w}. \quad [28]$$

The residual between Eq. [28] and the actual value of w_L is within 1% over the Lorentzian region ($a > 1$). The residual increases in the Gaussian region ($a < 1$) to within 3.4% at $a = 0.15$ and then increases sharply thereafter.

Recalling that $w_L = 1/\pi T_2$, from Eq. [28] we have an expression for T_2 given as

$$T_2 = \frac{w}{\pi(w^2 - w_G^2)}. \quad [29]$$

The usefulness of Eqs. [26] and [28] (obtained from the fitted parameters r and w) to routinely return the widths of the line broadening component w_G , and the intrinsic Lorentzian component w_L (and hence and T_2 values) of experimental line shapes is critically dependent on a fitting routine that returns parameter values which accurately represent the nature of the line shapes. This is especially so with the fractional parameter r , which governs the relative amounts

of Lorentzian and Gaussian contributions to the model function. This parameter must accurately represent the effectiveness of the shimming procedure (and hence the Voigt parameter a) and when fitting noiseless, single-peak spectra of differing Voigt profiles, the routine was found to adjust r in accordance with a (Fig. 5). On these simulated spectra, Eq. [29] proved to be useful only over the Lorentzian region, where the accuracy was within 1% up to $a = 5$, falling to 14.5% when $a = 1.05$.

In our *in vivo* work using single-voxel spectroscopy, cubic volumes of interest have been localized in the parietal white matter of patients and healthy volunteers by using PRESS with an echo time of 135 ms. In addition to studies on the line shape of the lactate doublet (13, 14), we have concentrated on the quantification of choline, creatine, and N-acetyl-aspartate, since these metabolites are well presented above baseline noise for long echo time acquisitions. Use of Eq. [29] to determine T_2 values of noiseless simulations of these three peaks again proved to be useful only over the Lorentzian region. The initially 100% Lorentzian peaks ($a = \infty$) when gradually broadened (a decreasing), resulted in an accuracy within 1% up to $a = 5$ falling to 20, 10, and 14% for each peak, respectively, when $a = 1$. In all cases however, the peak areas were accurately determined.

In our previous literature (1), we used linear combinations of Lorentzian and Gaussian functions of unit amplitude, and in that case the fractional parameter (r') has a different interpretation than the r used in functions of unit area

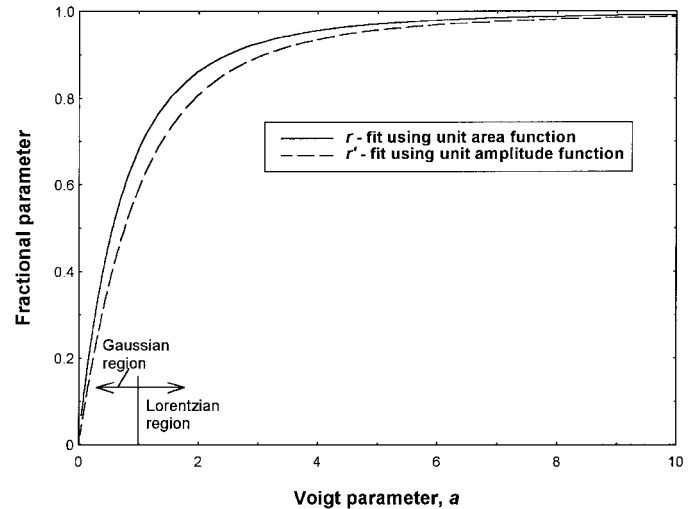


FIG. 5. The fractional parameter accurately reflects the nature of line shapes: The fitting routine adjusts r (the relative amounts of the Lorentzian and Gaussian contributions to the model) in accordance with a (the relative amounts of the Lorentzian and Gaussian contributions to the line shape), on simulated, noiseless, single-peak spectra of varying Voigt profiles. The fractional parameter returned when fitting with a unit amplitude function (r') is plotted for comparison.

(Fig. 5). The relationship between r and r' can be shown to be

$$r = \frac{r'}{\left[\frac{1}{\sqrt{\pi \ln 2}} + r' \left(1 - \frac{1}{\sqrt{\pi \ln 2}} \right) \right]}. \quad [30]$$

CONCLUSIONS

A derivation of an approximation to the Voigt function consisting of a linear combination of Lorentzian and Gaussian functions of equal width is presented. The derivation given is limited to the range of Voigt line shapes which are either predominantly Lorentzian or Gaussian in nature. It would be of interest, however, to extend this to include values of a close to 1. None the less, use of the approximation as a model function results in peak areas that are accurate to within 0.72% over the entire range of the Voigt parameter. With an empirical analysis of the approximation, we have shown that the direct recovery of T_2 values from line shapes is restricted to peaks that are predominantly Lorentzian.

REFERENCES

1. I. Marshall, J. Higinbotham, S. D. Bruce, and A. Freise, Use of Voigt lineshape for quantification of in vivo ^1H spectra, *Magn. Reson. Med.* **37**, 651–657 (1997).
2. A. Freise, E. Spencer, I. Marshall, and J. Higinbotham, A comparison of frequency and time domain fitting of ^1H MRS metabolic data, *Bull. Magn. Reson.* **17**, 302–303 (1995).
3. J. F. Kielkopf, New approximation to the Voigt function with appli-

cations to spectral-line profile analysis, *J. Opt. Soc. Am.* **63**, 987–995 (1973).

4. H. C. van de Hulst and J. J. M. Reesinck, Line breadths and Voigt profiles, *Astrophys. J.* **106**, 121 (1947).
5. A. B. McLean, C. E. J. Mitchell, and D. M. Swanston, Implementation of an efficient analytical approximation to the Voigt function for photoemission lineshape analysis, *J. Electron Spectrosc. Relat. Phenom.* **69**, 125–132 (1994).
6. K. Unterforsthuber and K. Bergmann, Mathematical separation procedure of broadline proton NMR spectra of crystalline polymers into components, *J. Magn. Reson.* **33**, 483–495 (1978).
7. J. P. Grivet, Accurate numerical approximation to the Gauss-Lorentz lineshape, *J. Magn. Reson.* **125**, 102–106 (1997).
8. G. K. Wertheim, M. A. Butler, K. West, and D. N. E. Buchanan, Determination of the Gaussian and Lorentzian content of experimental line shapes, *Rev. Sci. Instrum.* **45:11**, 1369–1371 (1974).
9. E. E. Whiting, An empirical approximation to the Voigt profile, *J. Quant. Spectrosc. Radiat. Transfer.* **8**, 1379–1384 (1968).
10. S. D. Bruce, I. Marshall, J. Higinbotham, and P. H. Beswick, The application of a numerical approximation of the Voigt function to synthetically generated MRS data, *In "Book of abstracts", 13th European Experimental NMR Conference, Paris, May 1996*, p. 346.
11. P. A. Jansson, "Deconvolution with Applications in Spectroscopy," p. 23, Academic Press, Orlando (1984).
12. W. H. Press, S. A. Teukolsky, and W. T. Vetterling, B. P. Flannery, "Numerical Recipes in C: The Art of Scientific Computing," 2nd Edition, p. 683, Cambridge Univ. Press, Cambridge, UK (1992).
13. I. Marshall and J. M. Wild, Calculations and experimental studies of the line shape of the lactate doublet in PRESS-localized ^1H MRS, *Magn. Reson. Med.* **38**, 415–419 (1997).
14. I. Marshall and J. M. Wild, A systematic study of the lactate line shape in PRESS-localized proton spectroscopy, *Magn. Reson. Med.* **40**, 72–78 (1998).